Tree crown economics

Brenden E McNeil[1*], Robert T Fahey[2], Christopher J King[1], Dara A Erazo[1], Ty Z Heimerl[1], and Andrew J Elmore[3]

Trees respond to global change in myriad ways, many of which may be linked to adaptations relating to tree crown architecture. However, there is a paucity of theory capable of predicting the adaptive importance and dynamics of crown architecture, most likely because of the difficulties involved in measuring the three-dimensional arrangement and orientation of tree leaves within individual crowns. Here, we describe a theory of tree crown economics, and use measurements from new lidar (light detection and ranging) instruments, UAVs (unoccupied aerial vehicles), and time-lapse camera imagery to identify support for two predictions of the theory, that (1) a light competition versus water use economic trade-off drives covariance among three tree crown functional traits (mean leaf angle, crown density, and crown rugosity), and (2) crown traits can drive spatial and temporal variability in near-infrared spectral reflectance and related ecosystem functions. Tree crown economic theory can complement leaf economic theory in helping ecologists map and model forest ecosystem responses to global change.

Front Ecol Environ 2023; 21(1): 40–48, doi:10.1002/fee.2588

Theoretical paradigms of leaf economics and leaf functional traits have led to transformative advances in our ability to not only succinctly represent the key adaptive trade-offs affecting the form and function of plant leaves, but also scale-up traits to forecast many ecosystem responses to drivers of global change (Reich 2014). Indeed, remotely sensed maps of leaf traits reveal many fascinating patterns in how the nutrient and structural investments into sunlit leaves vary in response to such diverse drivers such as carbon dioxide fertilization, land-use history, and nitrogen (N) deposition (eg see maps in Wang *et al.* [2020]). Yet, trees are much more than leaves. Especially when combined with coincident light detection and ranging (lidar)-based canopy structure measurements, interpretation of patterns on remotely sensed maps of leaf traits underscores the need to innovate theory and mapping methods to assess whole-crown responses to global changes such as droughts and altered species composition (Díaz *et al.* 2016; Kamoske *et al.* 2020). Specifically, we have limited capacity to predict how trees adaptively build the crown architectures that directly affect the light, temperature, and water microclimates controlling the carbon return on leaf investments (Hikosaka *et al.* 2016).

In a nutshell:

- Crown architecture is a key tree adaptation, and can govern forest responses to global change
- New imagery derived from lidar, UAVs, and time-lapse cameras aid measurement of crown architectural traits
- A light competition versus water use economic trade-off appears to drive differences in crown architecture among species, resulting in covariation among three crown traits: namely, mean leaf angle, crown density, and crown rugosity
- Crown traits drive spatial and temporal variability in near-infrared spectral reflectance, even within a season as trees adjust mean leaf angle
- A trait-based theory of tree crown economics can augment leaf economic theory in aiding predictions of forest responses to global change

Evolving in concert with leaf traits, tree crown architecture – defined here as the three-dimensional (3D) arrangement and orientation of leaves in an individual tree crown – is the form adapted by each tree to simultaneously compete for light, maximize carbon gain, and minimize respiration and water loss (Horn 1971; Ollinger 2011). By focusing on the carbon, light, and water economic trade-offs controlling tree crown architecture, we respond to renewed calls to innovate theory on "plant structural economics" (eg Díaz *et al.* 2016; Verbeeck *et al.* 2019). We focus on the orientation and arrangement of leaves on trees in closed-canopy forest systems. Particularly for plants that have evolved crown architectures within more open (eg savanna) systems, there may be additional adaptive traits regarding the overall crown size and horizontal crown shape (Verbeeck *et al.* 2019). In addition, other adaptive traits control the realized shape of a tree because of vascular, hydraulic, and mechanical trade-offs to branches and trunks (Verbeeck *et al.* 2019). We use the phrase "tree crown architecture" instead of "structure" to distinguish our emphasis on the 3D adaptations of individual tree crowns rather than the vertical cross-section descriptions of multiple crowns (and gaps) in a forest, which are the increasing focus of research on forest structure (eg Fahey *et al.* 2019). Metrics derived from these canopy

[1]*Department of Geology and Geography, Eberly College of Arts and Sciences, West Virginia University, Morgantown, WV* [*]*(brenden.mcneil@mail.wvu.edu);* [2]*Department of Natural Resources and the Environment and Center for Environmental Sciences and Engineering, University of Connecticut, Storrs, CT;* [3]*Center for Environmental Science, Appalachian Laboratory, University of Maryland, Frostburg, MD*

structures have great utility in correlating to ecosystem-level functions (such as light-use efficiency) while also revealing the impacts of past disturbance dynamics or the biophysical limiting factors acting on whole forests (Fahey *et al.* 2019). However, in comparison to the snapshot in time of an emergent structure of a forest canopy (eg with strong random components of gaps from disturbances and age structure from recruitment and mortality), the arrangement and orientation of leaves in individual tree crowns is shaped by short-term biotic acclimations and long-term species adaptations. Tree crown architecture therefore shapes how trees and forests respond to ongoing global change.

Why a trait-based theory of crown economics?

Past difficulties in directly measuring crown architecture (for instance, see the ingenious and enormous effort involved in analog measurements by Aber [1979] and Hutchison *et al.* [1986]) have left a scarcity of data to quantify differences among tree species, and even less data on how species may adjust their architecture (eg by altering leaf area or leaf angles) in response to their environment (Smith *et al.* 2019). Even in the comparatively well-studied system of temperate broadleaf deciduous forests, this scarcity of data continues to hinder our ability to test models and theories of coordinated leaf- and crown-level responses to environmental conditions (Hikosaka *et al.* 2016). Nevertheless, recent advances in embedded sensors and imaging capabilities, particularly from unoccupied aerial vehicles (UAVs) (McNeil *et al.* 2016) and lidar (Kellner *et al.* 2019), now provide rich data sources that can begin to approach the ideal of creating a dynamic, high-fidelity digital twin of a tree's architecture and functioning.

By extending and enhancing crown architectural observations made across the globe for decades (and indeed centuries, in some cases) by natural historians and ecologists (see eg Horn 1971; Pastor 2016), recent advances in technology can help to identify a more formal, functional trait-based theory of crown economics. Rigorous testing of this theory could promote at least two major advances for ecologists and resource managers: (1) crown functional traits can provide a powerful means to refine and test whole-crown models of photosynthesis and resource allocation, especially under current and future scenarios of global change; and (2) trait-based approaches can foster enhanced opportunities for remotely quantifying variability in crown architecture, thereby dramatically improving our ability to link ecosystem functioning to satellite-measured spectral reflectance.

Form/ trait	Tower	Pagoda	Dome
Leaf angle	Vertical	Vertical	Horiz.
Density	Low	High	High
Rugosity	High	High	Low

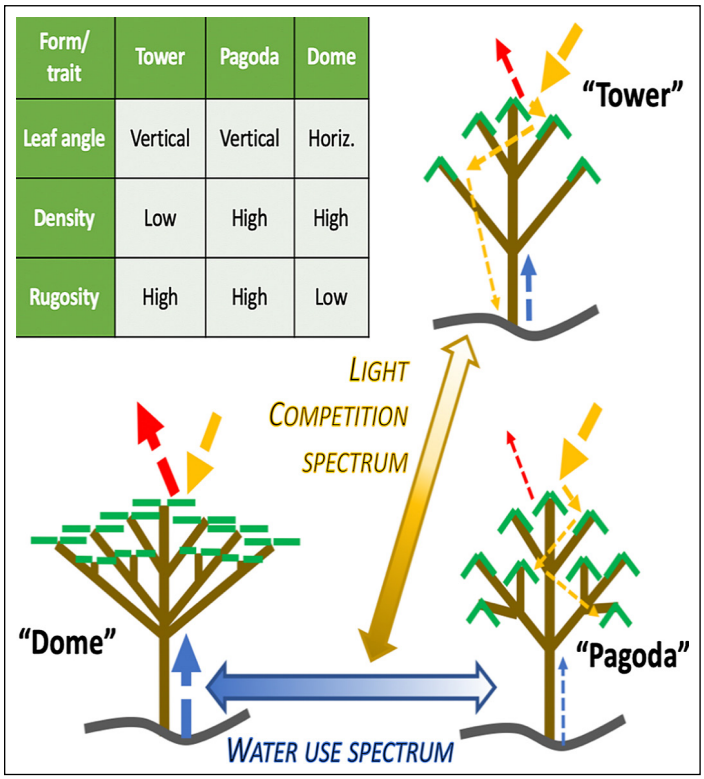

Figure 1. Three crown architectural endpoints ("tower", "dome", and "pagoda") resulting from economic trade-offs of light harvesting and water use, and defined by covariation in three crown traits (mean leaf angle, crown density, and crown rugosity), as depicted in the inset table. Arrow size illustrates the theorized effects of architecture on relative fluxes of sunlight (yellow arrows), near-infrared (NIR) spectral reflectance (red arrows), and water (blue arrows).

Revisiting "the adaptive geometry of trees" with trait-based economic theory

Classic works such as Horn's (1971) monograph "The adaptive geometry of trees", as well as contemporary crown-scale photosynthesis models (Hikosaka *et al.* 2016), suggest that there are several possible, but not always optimal, evolutionary stable states for arranging and orienting leaves in a tree crown. Moreover, texts describing plant resource strategies (eg Craine 2009), as well as studies describing crown architectural changes along successional (Horn 1971; Aber 1979), moisture and site quality (Horn 1971; Aber *et al.* 1982; Falster and Westoby 2003), elevation (Ehleringer 1988), and latitudinal gradients (Cohen and Pastor 1996), suggest that the crown economic strategies of trees likely fall along two orthogonal spectrums: the first defined by the strategy to compete for light and the second by the strategy for using water (Figure 1). As discussed in Panel 1 and depicted in Figure 2, these two crown economic spectrums based on light competition and water use are complementary to the nutrient-based leaf economics spectrum (Wright *et al.* 2004).

As one endpoint on the light competition spectrum, early successional trees use abundant light resources to array production-oriented leaves on sparse crowns with a "tower" architectural form (Figure 1). In the race upward for light, casting shade on competitors is not adaptive, and so trees orient leaves with more vertical leaf angles to prevent overheating and provide optimal partial shade, such

Panel 1. Generality of tree crown economics

Taken together, the light competition and water use spectrums of crown economics complement, but are independent from, the nutrient economic spectrum of leaf economics. Indeed, crown economics could guide ontogenetic, plastic, or ecotypic variation in the crown architecture within a species, or across species with very different leaf economic strategies. For instance, despite their varying crown architectures, the three species in the top panel of Figure 2 share a production-oriented strategy for investing nutrients into their broadleaf deciduous leaves. Moreover, there is similar divergence in the crown architectures of three persistence-oriented needleleaf evergreen species that are also abundant in eastern North America (Figure 2, bottom panel). Consistent with their known shade tolerances (Burns and Honkala 1990) and soil moisture preferences (Canham *et al.* 2006), the sparse crowns of a white pine (*Pinus strobus*) and big-tooth aspen (*Populus grandidentata*) both suggest a "tower" crown architecture, whereas the later-successional red spruce (*Picea rubens*) and black oak (*Quercus velutina*) have a more dense, multilayered "pagoda" form with more vertical leaf angles (O'Connell and Kelty 1994). Finally, the mesic eastern hemlock (*Tsuga canadensis*) and sugar maple (*Acer saccharum*) tend toward a "dome" architecture featuring horizontal leaves on a mono-layered crown (Horn 1971). Just as the covarying leaf economic traits of these species span much of the global spectrum of strategies for investing nutrients into leaves (Wright *et al.* 2004), the varied light and water resources within their realized ecological niches are likely to drive strong but coherent variability in their crown economic strategies.

Convergence of leaf and tree crown economics

Although leaf and crown economics offer conceptually independent theories for predicting plant responses to different types of global change, empirical evidence suggests there is convergence in leaf and crown traits (Ollinger 2011) that may be expressed within and across species, and even with ontogeny. This convergence is likely linked to complementary abiotic and biotic mechanisms. On the abiotic side, all trees have adapted to environments with strong covariation in their three primary resources: light, water, and nutrients. For instance, in higher latitudes or on poleward slope aspects, lower sun angles simultaneously reduce all three resources; not only is there less light, but decreased potential evapotranspiration also diminishes useful water availability, and cooler temperatures tend to slow rates of decomposition and the release of nutrients. Conversely, disturbance can increase the availability of all three primary resources (Craine 2009). On the biotic side, trees can coordinate their leaf and crown traits to effectively substitute one resource for another (Wright *et al.* 2003). As an example, trees with production-oriented leaf traits (eg high foliar nitrogen) may offset their lower photosynthetic nutrient-use efficiency by substituting excess light or water through a tower or dome crown architectural form (Figure 1) (Wright *et al.* 2003).

that most leaves operate near their light saturation point (Horn 1971; McMillen and McClendon 1979; Falster and Westoby 2003).

In contrast to the "tower" architectural endpoint on the light competition spectrum, the architecture of late successional trees differs according to their strategy for using water. At the mesic end of this water use spectrum, trees with "dome" architecture densely cluster more horizontally oriented leaves at the top of the crown (Hikosaka and Hirose 1997), which drives elevated near-infrared (NIR) spectral reflectance and albedo (see red arrows in Figure 1; Asner 1998; Ollinger 2011), along with higher potential carbon gain (Baldocchi *et al.* 2020) and evapotranspiration (Guerrieri *et al.* 2016). This "dome" crown form is also highly adaptive for casting deep shade on competitors (Givnish 1988; Canham *et al.* 1994). However, these advantages come with two distinct drawbacks. First, the high proportion of horizontal sunlit leaves in "dome" architectures makes them highly demanding of water (blue arrows in Figure 1), which greatly reduces water use efficiency (ie carbon gain per unit water) and often requires trees to close stomata and greatly curtail production during dry periods (Brzostek *et al.* 2014). Second, the adaptation to cast shade on competitors in mono-layered crowns (Horn 1971) often offsets any advantage of modulating leaf angles as a strategy to activate lower crown layers and reduce evapotranspiration during periods of low water availability.

Finally, a multilayered "pagoda" crown architectural form (Figure 1) is most adaptive in late successional environments where low solar radiation or water availability limit actual evapotranspiration. Under these conditions, trees increase water use efficiency and whole-crown light harvesting by densely arraying more vertically oriented leaves throughout their crowns (Horn 1971; Ehleringer 1988; Cohen and Pastor 1996). Although this strategy is the hallmark of the dense, conical crowns of needleleaf evergreen trees (Sprugel 1989), it is also adaptive in dry broadleaf forests (Hutchison *et al.* 1986; King 1997). Within these broadleaved forests, there appears to be a considerable advantage to respond to low water availability by increasing leaf angles in the upper sunlit crown, likely through a mechanism of hyponastic growth of leaf petioles (van Zanten *et al.* 2010). Such dynamic control of sunlit leaf angles could enable the comparatively cooler and more shaded leaves in lower crown layers to continue production during periods of water stress.

Testing tree crown economics

Do tree crown traits covary, and therefore provide evidence of economic trade-offs?

Just as strong covariation among leaf traits (eg %N, leaf mass per area, leaf longevity) describes the economic trade-offs controlling nutrient investment into leaves (Wright

et al. 2004), strong covariation among crown traits can serve as evidence for the economic trade-offs that trees face as they acclimate or adaptively arrange leaves to compete for light and use water. As detailed in the inset table in Figure 1, we tested for an expected pattern of covariation among three crown traits that affect the fitness and functioning of a tree; these traits are precisely defined by how each trait can be measured: (1) *Mean leaf angle* – the mean of at least 60 leaf angles measured on sunlit leaves in a crown. This trait evaluates the trade-off of casting shade versus permitting sunlight into the crown. (2) *Crown density* – the mean vegetation area index (VAI) measured within 1-m voxels systematically sampled by lidar throughout an individual tree crown. This trait assesses the investment in total leaf area, and represents the vertically summed leaf area index (LAI) for a tree crown. (3) *Crown rugosity* – The vertical variance in VAI throughout the crown. This trait evaluates investments in sun versus shade leaves, and helps describe the leaf area distribution for a tree crown.

We collected two initial datasets that strongly support the idea that these three crown traits can define the position of any individual tree on the two theorized spectrums of tree crown economics. In the first dataset (Figure 3), we used established methods to quantify traits of crown density and rugosity from vertical profiles collected from a portable canopy lidar instrument (Parker *et al*. 2004; Atkins *et al*. 2018). These profiles were taken from closed-canopy single-species plantations of three species whose niche strategies span the two spectrums of crown economics (Figure 3). As expected, the early successional tulip tree (*Liriodendron tulipifera*) has leaves sparsely and evenly distributed throughout the crown, resulting in a low crown density, but high crown rugosity (Figure 3). Next, the mesic, late successional sugar maple (*Acer saccharum*) has many leaves clustered near the top of the crown, resulting in high crown density, but low crown rugosity. Finally, the late successional but less mesic

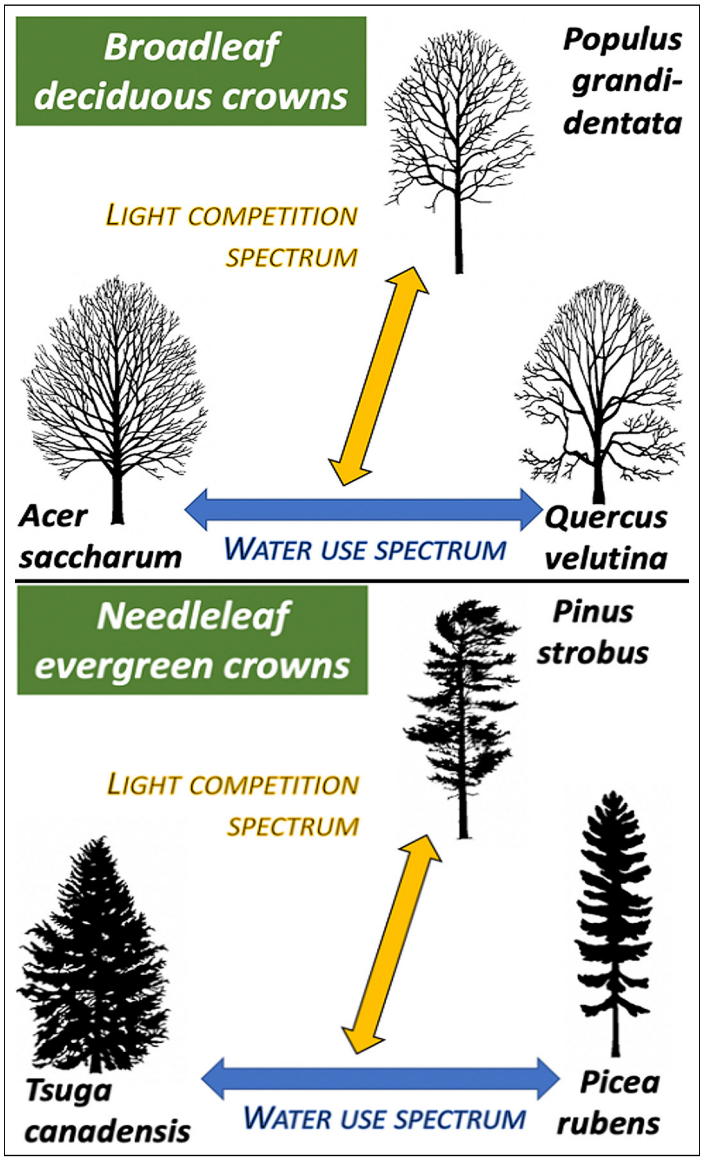

Figure 2. Examples of the "tower", "dome", and "pagoda" endpoint crown architectural forms for (top) common broadleaf deciduous and (bottom) needleleaf evergreen tree species in eastern North America, arrayed as in Figure 1. Tree silhouettes from Natural Resources Canada.

Crown trait	Litu	Quru	Acsa
Leaf angle (°)	68.4	57.2	28.5
Density (m^2/m^2)	2.9	3.6	5.4
Rugosity (m^2/m^2)	28.1	29.1	12.0

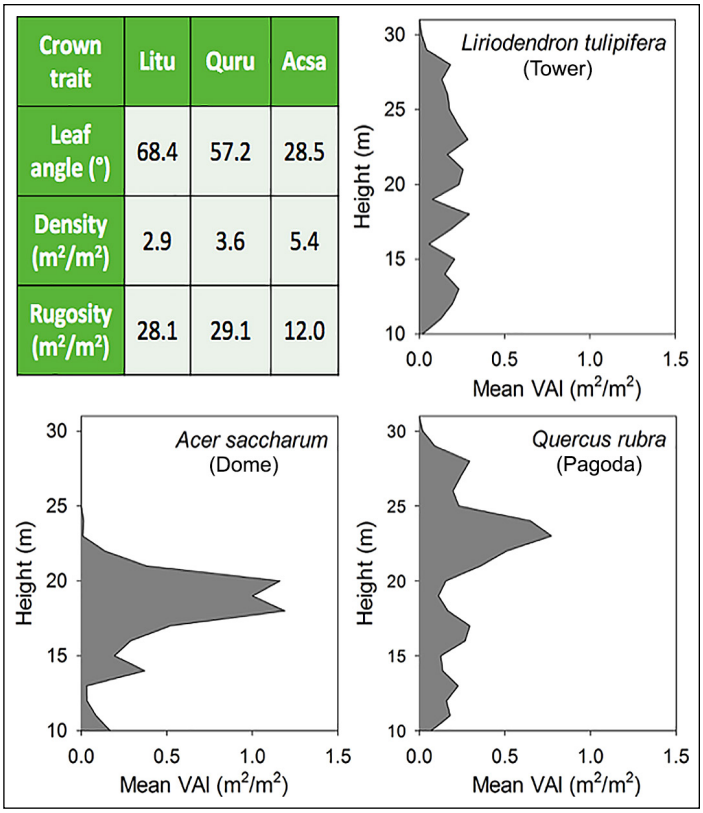

Figure 3. Light detection and ranging (lidar)-derived vertical distribution of leaf area for three species, arranged by their niche strategies along the crown economic spectrums shown in Figure 1. Vegetation area index = VAI. The inset table is also arranged as in Figure 1, but is populated with data summarizing the total leaf area (crown density) or variance in leaf area (crown rugosity). To complete the inset table, we include mean leaf angle data for each species (full data are in Figure 4). Scientific names and abbreviations: tulip tree (*Liriodendron tulipifera*, Litu), sugar maple (*Acer saccharum*, Acsa), northern red oak (*Quercus rubra*, Quru).

northern red oak (*Quercus rubra*) had both high crown density and high crown rugosity.

In the second dataset (Figure 4), we used the leveled photograph method (Ryu *et al.* 2010; McNeil *et al.* 2016) to measure leaf angles from walk-up towers and UAVs. For this crown-specific approach, we used a digital protractor to measure the angle from zenith to the leaf normal of at least 60 sunlit leaves that are oriented parallel to the plane of the image. These leaf angle data offer strong initial support for crown economic theory because the data match species niches defined by shade tolerance (Burns and Honkala 1990) and water availability (Canham *et al.* 2006). Crucially, when considered together, these initial lidar and leaf angle datasets exhibit strong agreement with our theoretical expectation that each species has adapted a crown economic strategy whereby the total amount and distribution of leaves in the crown covaries with the mean angle of leaves in the crown (see data in the inset table of Figure 3).

Testing the effects of crown traits on ecosystem functioning

The measurement of crown traits can also be useful for disentangling the convergent effects of leaf and crown traits on NIR spectral reflectance (Ollinger 2011), which is strongly and mechanistically related to ecosystem functions of albedo, evapotranspiration, and productivity (Guerrieri *et al.* 2016; Badgley *et al.* 2019; Baldocchi *et al.* 2020). By focusing on two separate patterns of NIR spectral reflectance, we have found evidence that the crown trait of mean leaf angle can drive important, multi-scale variability in ecosystem functioning through both space and time.

Species differences in mean leaf angle help explain the central Appalachian "climate coolspot"

To begin examining the role of crown traits in driving spatial variability in ecosystem functioning, we collected leaf angle data throughout a striking spatial pattern that we call the "climate coolspot" of elevated albedo, NIR reflectance, evapotranspiration, and C uptake in the central Appalachian Mountains (Figure 5) (Ollinger *et al.* 2008; Guerrieri *et al.* 2016). In particular, we accessed the sunlit crowns of the region's tree species through visiting existing walk-up towers in the region (typically abandoned fire towers) and by employing UAV methods (McNeil *et al.* 2016) to measure mean leaf angle in locations without walk-up towers, particularly in the wet and biodiverse Fernow Experimental Forest in West Virginia (Figure 5). Through all these measurements, we discovered that sugar maple crowns had significantly more horizontal leaf angles than

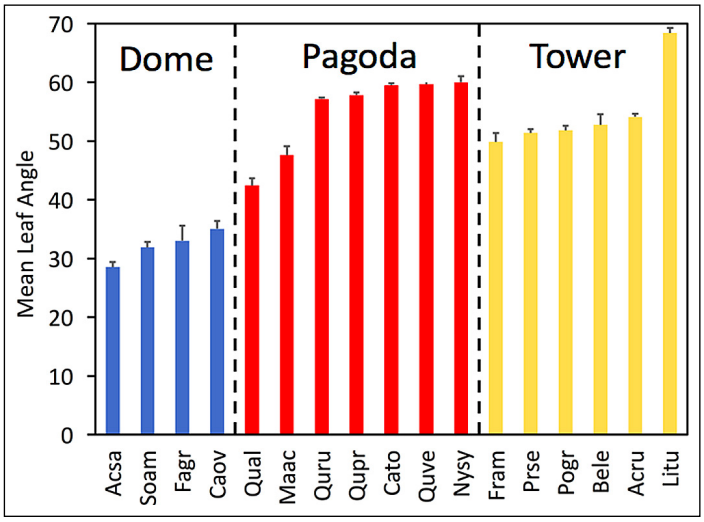

Figure 4. Species averages from 11,836 sunlit leaf angle observations within 20 sites throughout eastern North America. Taxa are named by the first two letters of their genus and species, and are placed along the water use and light competition spectrums in Figure 1 by known niche habitats (see main text). Error bars indicate standard errors.

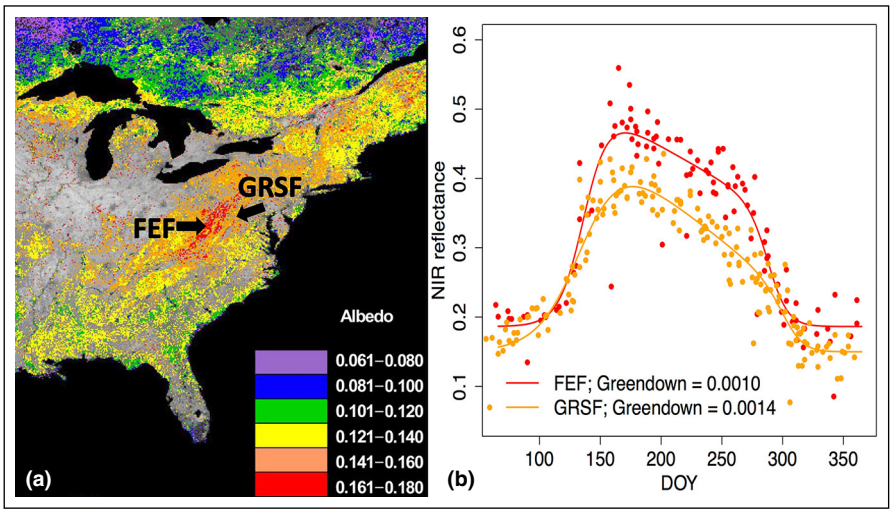

Figure 5. (a) The spatial pattern of shortwave albedo in eastern North America, adapted from Figure 4 in Ollinger *et al.* (2008) (© The National Academy of Sciences of the USA). This "climate coolspot" spatial pattern of elevated albedo is centered on the USDA Forest Service Fernow Experimental Forest (FEF) in the central Appalachian Mountains, and is driven by elevated near-infrared (NIR) reflectance, which corresponds to higher rates of carbon uptake (leaf-level photosynthetic capacity or A_{max}) (Ollinger *et al.* 2008) and evapotranspiration (Guerrieri *et al.* 2016). (b) Landsat phenology data (see Elmore *et al.* [2012] for methods) align with the moderate resolution imaging spectroradiometer (MODIS)-derived satellite map of Ollinger *et al.* (2008), showing that a dry, closed-canopy oak/hickory (*Quercus*/*Carya* spp) forest (with "pagoda" crown architectures) in the Green Ridge State Forest (GRSF) in Maryland has a lower maximum NIR reflectance than the sugar maple (*Acer saccharum*) ("dome" architecture)-dominated forest in the mesic FEF site. The Landsat phenology data in (b) also suggest a higher rate of NIR greendown in the GRSF, which appears to be driven by mean leaf angle values that become increasingly vertical through the summer (Figure 7) (Reaves *et al.* 2018). Day of the year = DOY.

other species (eg see data in Figures 3 and 4). At the FEF site, we also mounted a multispectral camera (Tetracam ADC Snap; Chatsworth, CA) to the UAV to obtain top-down views, which revealed that sugar maple crowns had much higher and more uniform NIR brightness than surrounding trees (Figure 6). Then, using both high-resolution multispectral satellite imagery and the intensity of returns from the NIR laser beams of airborne leaf-on lidar data, we confirmed that the mesic, late-successional sugar maple crowns have significantly higher NIR reflectance than all other species in the Fernow Experimental Forest (Fang *et al.* 2018).

Given the increasing and often dominant abundance of sugar maple throughout the central Appalachian Mountains (Schuler and Gillespie 2000), we suggest that much of the "climate coolspot" spatial pattern of forest functioning visible in Figure 5 might be explained by the relative abundance of sugar maple and other tree species with a "dome" architecture (Figure 1). Indeed, as an initial test, we found that our species-specific mean leaf angle values (Figure 4), weighted by the relative abundance of tree species in 254 US Department of Agriculture Forest Service Forest Inventory and Analysis (FIA) plots in the central Appalachian region, could explain a significant amount of the plot-level variation (R^2 = 0.12, $P < 0.0001$) in maximum NIR reflectance measured from Landsat phenology data (Figure 5b) (following methods described by Elmore *et al.* [2012]). In fact, these plot-scaled mean leaf angle estimates explained more variation in maximum NIR reflectance than did abiotic drivers such as slope, aspect, and elevation. On the basis of this example of the "climate coolspot" in the central Appalachian Mountains, we encourage conducting additional tests, ones that more directly focus on disentangling the roles of leaf and crown traits in driving multi-scale spatial patterns of NIR reflectance and ecosystem functioning.

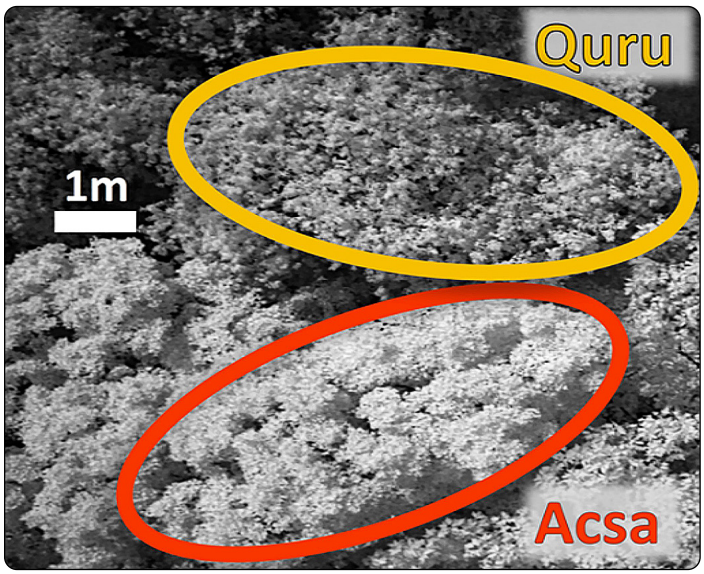

Figure 6. Species differences in crown near-infrared (NIR) brightness measured from instruments on an unoccupied aerial vehicle (UAV) deployed in the Fernow Experimental Forest, West Virginia. Relative to the patchy and lower NIR brightness (darker pixels) in the northern red oak (*Quercus rubra*, Quru) crown, the more intense (brighter pixels) and uniform pattern in sugar maple (*Acer saccharum*, Acsa) is expected from its crown traits (Figure 3).

Leaf angle phenology can drive NIR greendown

We have also examined the relationship between crown traits and a widely observed temporal pattern called NIR greendown, or declining NIR reflectance between early and late summer (Figure 5b) (Elmore *et al.* 2012). We previously used manual repeat photography to suggest that plant-directed control of leaf angle (that is, leaf angle phenology; for discussions concerning likely plant physiological mechanisms, see McMillen and McClendon [1979], King [1997], and van Zanten *et al.* [2010]) was the most likely cause of Landsat-observed greendown in the Green Ridge State Forest (GRSF), a dry, closed-canopy oak (*Quercus* spp) and hickory (*Carya* spp) forest in western Maryland (Figure 5) (Reaves *et al.* 2018). To confirm this finding, we used an abandoned fire tower at an especially dry ridgetop site in the GRSF to measure greendown from (1) boom-mounted light sensors measuring the normalized difference vegetation index (NDVI) of the canopy immediately under the tower (Figure 7, a and b), following methods described in Jenkins *et al.* (2007); and (2) a solar-powered, cellular-networked NIR phenocam ("Greenridge1" within the PhenoCam dataset [v2.0]) (Seyednasrollah *et al.* 2019) used to measure crown-specific NDVI phenology (NDVI from methods in Petach *et al.* [2014]; see example results for a black oak [*Quercus velutina*] crown in Figure 7, a and c). By relating these NIR greendown measurements to leaf angle data measured on the same crowns from automated time-lapse cameras mounted at heights level with the sunlit crowns of three tree species (Figure 7, d and e), we found strong support for the theory that increasingly vertical leaf angles can drive NIR greendown. For instance, the average of mean leaf angle values from the three species (data in Figure 7e) predicted 60% of the variation (R^2 = 0.60, $P < 0.0001$) in NDVI measured by the light sensors (data in Figure 7b). That changes in mean leaf angle were directly responsible for the decline in NIR reflectance in the GRSF is supported by three lines of evidence: (1) the coincident timing of changes in leaf angle and spectral reflectance; (2) modeling work indicating that the changes in leaf angle are large enough to affect NIR reflectance (Asner 1998); and (3) our earlier work at the GRSF, in which we found that greendown was not correlated with changes in leaf-level spectral reflectance between June and August (Reaves *et al.* 2018). Although leaf angle appears to drive greendown in the GRSF, other, more mesic forests appear to have little

greendown, or may have other drivers of temporal variability in NIR reflectance (eg a change in crown density; Smith *et al.* 2019). For instance, we installed time-lapse cameras and analyzed leaf angle phenology in northern red oak and red maple (*Acer rubrum*) trees surrounding a walkup tower at the Harvard Forest in central Massachusetts in 2017, and observed little seasonal change in mean leaf angle, which is consistent with the relatively stable NIR reflectance and gross ecosystem production during the leaf-on period at this mesic site (Wehr *et al.* 2016). By repeating the coincident measurements of NIR and crown trait phenology at other sites, such as our ongoing measurements at National Ecological Observatory Network (NEON) towers in the eastern US, future research on NIR greendown can further identify the apparent species and site differences in how trees dynamically adjust their crown architectures to respond to global change and affect ecosystem functioning.

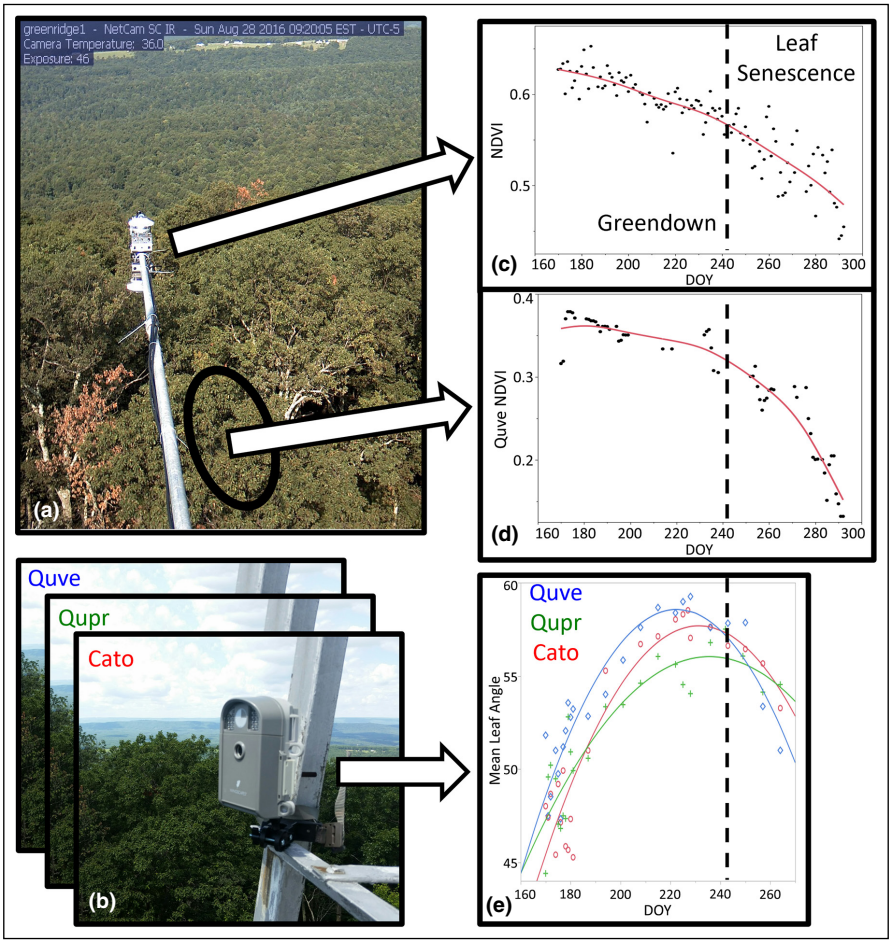

Figure 7. The phenologies of (a–c) NIR greendown and (d and e) leaf angle from a tower in the GRSF. (a) A phenocam image from the 241st day of the year (DOY; that is, DOY 241) in 2016 shows (b) the boom-mounted light sensors used to measure normalized difference vegetation index (NDVI) phenology of the multi-species forest canopy adjacent to the tower. (c) Analysis of phenocam data from one black oak (*Quercus velutina*, Quve) crown next to the tower shows a similar NDVI phenology, albeit with a more apparent decline in NDVI after DOY 241. Following DOY 241, the visible color imagery shows decreasing leaf greenness, suggesting that DOY 241 was likely the onset of leaf senescence. (d) Analysis of images from time-lapse cameras mounted lower on the tower, and level with sunlit crowns of three different species located under the boom, reveals (e) increasingly vertical leaf angles in black oak (Quve), chestnut oak (*Quercus prinus*, Qupr), and mockernut hickory (*Carya tomentosa*, Cato) between DOY 160 and DOY 241.

Conclusions

A trait-based crown economic theory can provide a valuable approach for explaining the crown-scale mechanisms that can drive many aspects of forest responses to global change. We tested two theoretical predictions of tree crown economics. First, through finding species niche separation and covariation among three crown traits (mean leaf angle, crown density, and crown rugosity), we found evidence that economic trade-offs among light harvesting and water use appear to drive variation in tree crown architecture. Second, we discovered that crown traits can mechanistically drive two heretofore poorly understood patterns in ecosystem functioning: the "climate coolspot" in the central Appalachian Mountains and NIR greendown phenology. By more rigorously testing the coordination of crown economic traits and by using NIR reflectance to mechanistically scale crown traits to ecosystem functioning, future research can open new avenues for: (1) measuring and mapping crown traits, including through the application of novel lidar-based approaches to automatically measure leaf angles (Stovall *et al.* 2021); (2) exploring the convergence of trait-based leaf economic and crown economic theories; (3) testing above- and belowground models of resource allocation; and (4) building a new class of trait-based models that can more robustly predict the future of forest functioning under ongoing rapid global change.

Acknowledgements

Financial support for this Special Issue was provided by the US National Science Foundation (NSF DEB award 1924942). We are indebted to the laborious contributions of West Virginia University undergraduate students to the leaf angle dataset, including B Anderson, E Flamenco, and S Rescorl. Generous support for this work has come from West Virginia University, the National Aeronautics and Space Administration West Virginia Space Grant

Consortium, the US Department of Agriculture (USDA) Forest Service (USFS), the NSF (DEB MSB-NES grant 2106080), and the Harvard Forest Bullard Fellowship to BEM. We also are grateful for public access to many fire towers, and for research access to the Green Ridge State Forest of Maryland, Harvard Forest, and the USFS Fernow Experimental Forest. Finally, we appreciate theoretical conversations, encouragement, technical help, and comments on early drafts from many individuals, especially E Brzostek, C Canham, M Duveneck, T Millman, S Ollinger, J Pastor, N Pederson, A Richardson, and T Warner.

Data Availability Statement

Leaf angle, lidar, and Landsat phenology datasets are archived in the Environmental Data Initiative.

References

Aber JD, Pastor J, and Melillo JM. 1982. Changes in forest canopy structure along a site quality gradient in southern Wisconsin. *Am Midl Nat* **108**: 256–65.

Aber JD. 1979. Foliage-height profiles and succession in northern hardwood forests. *Ecology* **60**: 18–23.

Asner GP. 1998. Biophysical and biochemical sources of variability in canopy reflectance. *Remote Sens Environ* **64**: 234–53.

Atkins JW, Bohrer G, Fahey RT, *et al*. 2018. Quantifying vegetation and canopy structural complexity from terrestrial LiDAR data using the forestr R package. *Methods Ecol Evol* **9**: 2057–66.

Badgley G, Anderegg LDL, Berry JA, and Field CB. 2019. Terrestrial gross primary production: using NIRV to scale from site to globe. *Glob Change Biol* **25**: 3731–40.

Baldocchi DD, Ryu Y, Dechant B, *et al*. 2020. Outgoing near infrared radiation from vegetation scales with canopy photosynthesis across a spectrum of function, structure, physiological capacity and weather. *J Geophys Res-Biogeo* **125**: e2019JG005534.

Brzostek ER, Dragoni D, Schmid HP, *et al*. 2014. Chronic water stress reduces tree growth and the carbon sink of deciduous hardwood forests. *Glob Change Biol* **20**: 2531–39.

Burns RM and Honkala BH. 1990. Silvics of North America. Washington, DC: USDA Forest Service.

Canham CD, Finzi AC, Pacala SW, and Burbank DH. 1994. Causes and consequences of resource heterogeneity in forests: interspecific variation in light transmission by canopy trees. *Can J Forest Res* **24**: 337–49.

Canham CD, Papaik MJ, Uriarte M, *et al*. 2006. Neighborhood analyses of canopy tree competition along environmental gradients in New England forests. *Ecol Appl* **16**: 540–54.

Cohen Y and Pastor J. 1996. Interactions among nitrogen, carbon, plant shape, and photosynthesis. *Am Nat* **147**: 847–65.

Craine JM. 2009. Resource strategies of wild plants. Princeton, NJ: Princeton University Press.

Díaz S, Kattge J, Cornelissen JHC, *et al*. 2016. The global spectrum of plant form and function. *Nature* **529**: 167–71.

Ehleringer JR. 1988. Changes in leaf characteristics of species along elevational gradients in the Wasatch Front, Utah. *Am J Bot* **75**: 680–89.

Elmore AJ, Guinn SM, Minsley BJ, and Richardson AD. 2012. Landscape controls on the timing of spring, autumn, and growing season length in mid-Atlantic forests. *Glob Change Biol* **18**: 656–74.

Fahey RT, Atkins JW, Gough CM, *et al*. 2019. Defining a spectrum of integrative trait-based vegetation canopy structural types. *Ecol Lett* **22**: 2049–59.

Falster DS and Westoby M. 2003. Leaf size and angle vary widely across species: what consequences for light interception? *New Phytol* **158**: 509–25.

Fang F, McNeil BE, Warner TA, and Maxwell AE. 2018. Combining high spatial resolution multi-temporal satellite data with leaf-on LiDAR to enhance tree species discrimination at the crown level. *Int J Remote Sens* **39**: 9054–72.

Givnish T. 1988. Adaptation to sun and shade: a whole-plant perspective. *Funct Plant Biol* **15**: 63–92.

Guerrieri R, Lepine L, Asbjornsen H, *et al*. 2016. Evapotranspiration and water use efficiency in relation to climate and canopy nitrogen in US forests. *J Geophys Res-Biogeo* **121**: 2016JG003415.

Hikosaka K and Hirose T. 1997. Leaf angle as a strategy for light competition: optimal and evolutionarily stable light-extinction coefficient within a leaf canopy. *Écoscience* **4**: 501–7.

Hikosaka K, Niinemets Ü, and Anten NPR (Eds). 2016. Canopy photosynthesis: from basics to applications. Dordrecht, the Netherlands: Springer.

Horn HS. 1971. The adaptive geometry of trees. Princeton, NJ: Princeton University Press.

Hutchison BA, Matt DR, McMillen RT, *et al*. 1986. The architecture of a deciduous forest canopy in eastern Tennessee, USA. *J Ecol* **74**: 635–46.

Jenkins JP, Richardson AD, Braswell BH, *et al*. 2007. Refining light-use efficiency calculations for a deciduous forest canopy using simultaneous tower-based carbon flux and radiometric measurements. *Agr Forest Meteorol* **143**: 64–79.

Kamoske AG, Dahlin KM, Serbin SP, and Stark SC. 2020. Leaf traits and canopy structure together explain canopy functional diversity: an airborne remote sensing approach. *Ecol Appl* **31**: e02230.

Kellner JR, Albert LP, Burley JT, and Cushman KC. 2019. The case for remote sensing of individual plants. *Am J Bot* **106**: 1139–42.

King DA. 1997. The functional significance of leaf angle in *Eucalyptus*. *Aust J Bot* **45**: 619–39.

McMillen GGM and McClendon JHM. 1979. Leaf angle: an adaptive feature of sun and shade leaves. *Bot Gaz* **140**: 437–42.

McNeil BE, Pisek J, Lepisk H, and Flamenco EA. 2016. Measuring leaf angle distribution in broadleaf canopies using UAVs. *Agr Forest Meteorol* **218–219**: 204–08.

O'Connell BM and Kelty MJ. 1994. Crown architecture of understory and open-grown white pine (*Pinus strobus* L) saplings. *Tree Physiol* **14**: 89–102.

Ollinger SV, Richardson AD, Martin ME, *et al*. 2008. Canopy nitrogen, carbon assimilation, and albedo in temperate and boreal forests: functional relations and potential climate feedbacks. *P Natl Acad Sci USA* **105**: 19336–41.

Ollinger SV. 2011. Sources of variability in canopy reflectance and the convergent properties of plants. *New Phytol* **189**: 375–94.

Parker GG, Harding DJ, and Berger ML. 2004. A portable LIDAR system for rapid determination of forest canopy structure. *J Appl Ecol* **41**: 755–67.

Pastor J. 2016. What should a clever moose eat? Natural history, ecology, and the North Woods. Washington, DC: Island Press.

Petach AR, Toomey M, Aubrecht DM, and Richardson AD. 2014. Monitoring vegetation phenology using an infrared-enabled security camera. *Agr Forest Meteorol* **195–196**: 143–51.

Reaves VC, Elmore AJ, Nelson DM, and McNeil BE. 2018. Drivers of spatial variability in greendown within an oak–hickory forest landscape. *Remote Sens Environ* **210**: 422–33.

Reich PB. 2014. The world-wide "fast–slow" plant economics spectrum: a traits manifesto. *J Ecol* **102**: 275–301.

Ryu Y, Sonnentag O, Nilson T, *et al*. 2010. How to quantify tree leaf area index in an open savanna ecosystem: a multi-instrument and multi-model approach. *Agr Forest Meteorol* **150**: 63–76.

Schuler TM and Gillespie AR. 2000. Temporal patterns of woody species diversity in a central Appalachian forest from 1856 to 1997. *J Torrey Bot Soc* **127**: 149–61.

Seyednasrollah B, Young AM, Hufkens K, *et al*. 2019. PhenoCam dataset v2.0: vegetation phenology from digital camera imagery, 2000–2018. Oak Ridge, TN: Oak Ridge National Laboratory.

Smith MN, Stark SC, Taylor TC, *et al*. 2019. Seasonal and drought-related changes in leaf area profiles depend on height and light environment in an Amazon forest. *New Phytol* **222**: 1284–97.

Sprugel DG. 1989. The relationship of evergreenness, crown architecture, and leaf size. *Am Nat* **133**: 465–79.

Stovall AEL, Masters B, Fatoyinbo L, and Yang X. 2021. TLSLeAF: automatic leaf angle estimates from single-scan terrestrial laser scanning. *New Phytol* **232**: 1876–92.

van Zanten M, Pons TL, Janssen JAM, *et al*. 2010. On the relevance and control of leaf angle. *Crit Rev Plant Sci* **29**: 300–16.

Verbeeck H, Bauters M, Jackson T, *et al*. 2019. Time for a plant structural economics spectrum. *Front Forest Glob Chang* **2**: 43.

Wang Z, Chlus A, Geygan R, *et al*. 2020. Foliar functional traits from imaging spectroscopy across biomes in eastern North America. *New Phytol* **228**: 494–511.

Wehr R, Munger JW, McManus JB, *et al*. 2016. Seasonality of temperate forest photosynthesis and daytime respiration. *Nature* **534**: 680–83.

Wright IJ, Reich PB, and Westoby M. 2003. Least-cost input mixtures of water and nitrogen for photosynthesis. *Am Nat* **161**: 98–111.

Wright IJ, Reich PB, Westoby M, *et al*. 2004. The worldwide leaf economics spectrum. *Nature* **428**: 821–27.